REPORT TO NRC ON THE EFFECT OF INSTALLING CORE REGION CONSTRAINT DEVICES ON THE SEISMIC RESPONSE OF THE FORT ST. VRAIN CORE

R. C. Dove
J. G. Bennett
C. A. Anderson

University of California
LOS ALAMOS SCIENTIFIC LABORATORY
Post Office Box 1663 Los Alamos, New Mexico 87545

INTRODUCTION

The Reactor and Advanced Heat Transfer Technology Group (Q-13) of the Los Alamos Scientific Laboratory (LASL), acting as consultants to the Nuclear Regulatory Commission, has examined the effects of the Public Service Company of Colorado's (PSC) proposal to install core region constraint devices (RCDs) onto the top plane of the Fort St. Vrain (FSV) core with regard to the seismic safety of the core. The devices are being considered for installation in an effort to solve a temperature fluctuation problem currently experienced at FSV under certain operating conditions. The questions that we have addressed are how the addition of the RCDs will affect the dowel shear forces and fuel element impact forces during a seismic event.

SUMMARY OF ANALYSIS

Because of the relatively low intensity levels of known and predicted earthquakes for the Fort St. Vrain region, and because of the relatively large values of coefficient of friction for graphite on graphite in a dry helium environment, the fuel regions will initially respond as top restrained cantilever columns excited at their base during a seismic event. Since we desire to know the relative effect of RCD installation upon maximum dowel shear forces and maximum impact forces during a seismic event, we have examined the effects of imposing two types of end restraint on a cantilever column undergoing seismic excitation. To facilitate the analysis we have used an available bottom head reactor horizontal response spectra corrected to one that we believe to be appropriate for the core support plane at the Fort St. Vrain plant. We have also used the horizontal response spectra for the Fort St. Vrain plant reactor and turbine building floor slabs. This response spectra includes the FSV PCRV motion but not the core support plane.

We have determined the possible extreme values of the lowest natural frequency of the fuel columns by including in the analysis such effects as bending, shear effects, geometric stiffness effects caused by both the fuel column weight and end loads, lateral pressure effects and irradiation material property changes. Table I shows the results of this analysis. By using the extreme bounding values of lowest natural frequency of the fuel columns (i.e., $\omega = 16\ s^{-1}$ and $\omega = 29\ s^{-1}$) and the response spectra, and by examining the relative stiffening effect of changing the end conditions

on the cantilever column from free to one that is simply supported or clamped , the relative effect of the RCD on dowel shear forces can then be predicted. Table II gives this result.

SUMMARY OF CONCLUSIONS

With regard to the seismic response of the Fort St. Vrain core, the addition of the RCDs can be expected to decrease the maximum dowel shear forces as shown in column 3 of Table II. One exception is noted. This exception involves FSV being a very "soft" (low natural frequency) or a very "hard" (high natural frequency) system. In these cases maximum shear forces could increase. Based on general knowledge of large massive structures of the FSV type, these exceptions are not deemed credible. For motions produced when fuel block slippage occurs, the fuel element impact velocities and impact forces will also be decreased.

In summary, the addition of the RCDs should serve to make the FSV core a more seismically safe structure.

TABLE I

FUEL COLUMN NATURAL FREQUENCIES (1/s)

Graphite Material Modulus H-327	ω_1	ω_2	ω_3	ω_4	ω_5
1.3×10^6 psi (unirradiated)	16.27	16.21	16.19	17.10	17.15
3.9×10^6 psi (irradiated)	28.19	28.15	28.14	28.68	28.93

where,

ω_1 - bending only

ω_2 - bending plus geometric stiffness due to weight

ω_3 - bending plus geometric stiffness due to weight and end loads

ω_4 - bending plus geometric stiffness and lateral pressure effects

ω_5 - bending plus geometric stiffness plus lateral pressure effects plus shear correction

TABLE II

EXPECTED CHANGE IN COLUMN MAXIMUM SHEAR FORCES

Case	Bounding natural frequency (rad/s)	Column maximum shear force
Case I (Cantilever column - i.e. <u>no</u> RCDs)	$\omega_I = 16$ $(T_I = 0.39$ s)	S_I
	$\omega_I = 29$ $(T_I = 0.22$ s)	S_I
Case II (RCDs produce fixed condition at top of column)	$\omega_{II} = 6.4 \times 16$ $= 102$ $(T_{II} = 0.06$ s)	Using Fig. 3 $S_{II} = 0.08\ S_I$ Using Fig. 4 $S_{II} = 0.47\ S_I$
	$\omega_{II} = 6.4 \times 29$ $= 185$ $(T_{II} = 0.03$ s)	Using Fig. 3 $S_{II} = 0.28\ S_I$ Using Fig. 4 $S_{II} = 0.19\ S_I$
Case III (RCDs produce pinned condition at top of column)	$\omega_{III} = 4.4 \times 16$ $= 70$ $(T_{III} = 0.09$ s)	Using Fig. 3 $S_{III} = 0.13\ S_I$ Using Fig. 4 $S_{III} = 0.58\ S_I$
	$\omega_{III} = 4.4 \times 29$ $= 127$ $(T_{III} = 0.05$ s)	Using Fig. 3 $S_{III} = 0.45\ S_I$ Using Fig. 4 $S_{III} = 0.99\ S_I$

APPENDIX
METHOD OF ANALYSIS

INTRODUCTION

Since it was assumed in the Final Safety Analysis Report (FSAR) for the FSV reactor that the core was restrained during seismic events and the analysis used involved the application of an equivalent static load to this "restrained" core it is not possible to extend this original analysis to determine how the addition of the RCDs will change the seismic loading on the individual core blocks.

A review of the FSAR reveals that for the FSV Nuclear Generating Station the Operating Basis Earthqake (OBE) is taken as 0.05 g horizontal and the Safe Shutdown Earthquake (SSE) is taken as 0.10 g horizontal. Further, dynamic analysis of the core support structure indicated that these ground accelerations result in accelerations at the core level of 0.19 g (OBE) and 0.26 g (SSE). At these relatively low acceleration levels the individual core blocks would not be expected to slip horizontally relative to each other until after an impact event. The reason for this is the fact that without some other driving force slippage does not occur until the base acceleration in "gs" is equal to or greater than the static coefficient of friction between blocks (graphite on graphite), and previous research indicates that this coefficient is greater than 0.2 and probably greater than 0.3.* From this observation it follows that during seismic excitation the stacked core blocks will respond first as a column rather than as individual blocks moving (slipping) relative to each other.

SIMPLIFIED BOUNDING ANALYSIS

Three cases will be considered to investigate the effect of adding the RCDs on the seismic response. Since we wish to examine the effect in terms of dowel shear forces, we need a method to estimate the ratio of the column shear forces in the new configuration as compared with the original

---

* Ref. 1 shows that the coefficient of kinetic friction of graphite on graphite is in excess of 0.3 in a dry, high temperature, helium envrionment. The static coefficient is known to be higher than the kinetic value.

configuration. Let the original configuration be represented by a cantilever beam with a unit lateral load applied at the end for which the statical deflections give a good approximation to the first mode shape of the beam. Using simple beam theory, we can show that relationship between the maximum shear force, S_I, and maximum deflection, Z_I, of the tip is

$$S_I = \frac{3EI}{L^3} Z_I .$$

where EI is the bending stiffness of the beam (The term $3EI/L^3$ is the commonly known spring stiffness for the cantilever). We define this approximation for the original configuration as case I.

With the addition of the RCDs, the fuel column will behave differently. Under the proper conditions it can behave as a beam clamped at both ends. An appropriate mode shape to estimate maximum shear forces is a beam fixed at both ends and loaded in the center which we will define as case II. For case II, the relationship between the maximum shear forces and the maximum deflection can be shown to be

$$S_{II} = \frac{192EI}{2L^3} Z_{II}.$$

The boundary condition at the RCD end of the column can also be approximated as a pinned condition which we define as case III. In case III,

$$S_{III} = 33\sqrt{5} \frac{EI}{L^3} Z_{III}$$

We can conclude that the relationship between maximum shear forces, S, developed in these cases are as follows

$$\frac{S_{II}}{S_I} = 32 \frac{Z_{II}}{Z_I} \quad \text{and} \quad \frac{S_{III}}{S_I} = 24 \frac{Z_{III}}{Z_I}$$

where Z_i are the maximum relative displacements. Furthermore, the ratios of the first mode natural frequencies for these cases are such that,*

$$\frac{\omega_{II}}{\omega_I} = 6.4 \quad \text{and} \quad \frac{\omega_{III}}{\omega_I} = 4.4.$$

The question to be answered is, "How will the stiffening (an increase in the natural frequency), affect the shear forces (s) developed during a seismic event.

The approach that we will use in answering this question can best be illustrated by assuming that the exciting function (x) is harmonic. Figure 1 taken from Ref. 3 shows the response curves for a horizontally base excited single degree of freedom system. Referring to Fig. 1 we can see that if the original system (case I) is relatively flexible (i.e. $\omega/\omega_n >> 1$, where ω is the forcing frequency), then increasing the stiffness (as in case II) will decrease the ratio of ω/ω_n. Such a decrease will result in an increase in the shear forces developed. As an example, assume $\omega/\omega_{n_I} = 10$ and h (the damping ratio) = 0.3. Then

$$\frac{\omega}{\omega_{n_{II}}} = 1.56$$

From Fig. 1,

$Z_I = X$, where X is the input displacement and $Z_{II} = 1.48\ X$. Then

$$\frac{S_{II}}{S_1} = 32 \times \frac{1.48}{1} \qquad \text{whereupon } S_{II} = 47\ S_I .$$

This example illustrates that the increase in shearing force can be quite severe under the proper conditions.

* For example, see Ref. 2.

On the other hand, if the original system (case I) is near resonance ($\omega/\omega_{n_I} = 1$) or already a "stiff" system ($\omega/\omega_1 < 1$) then increasing the stiffness will decrease the shear force developed. For example, using case III data for which

$$\frac{\omega_{n_{III}}}{\omega_{n_I}} = 4.4,$$

assume we have

$$\frac{\bar{\omega}}{\omega_{n_I}} = 1 \text{ and } h = 0.3$$

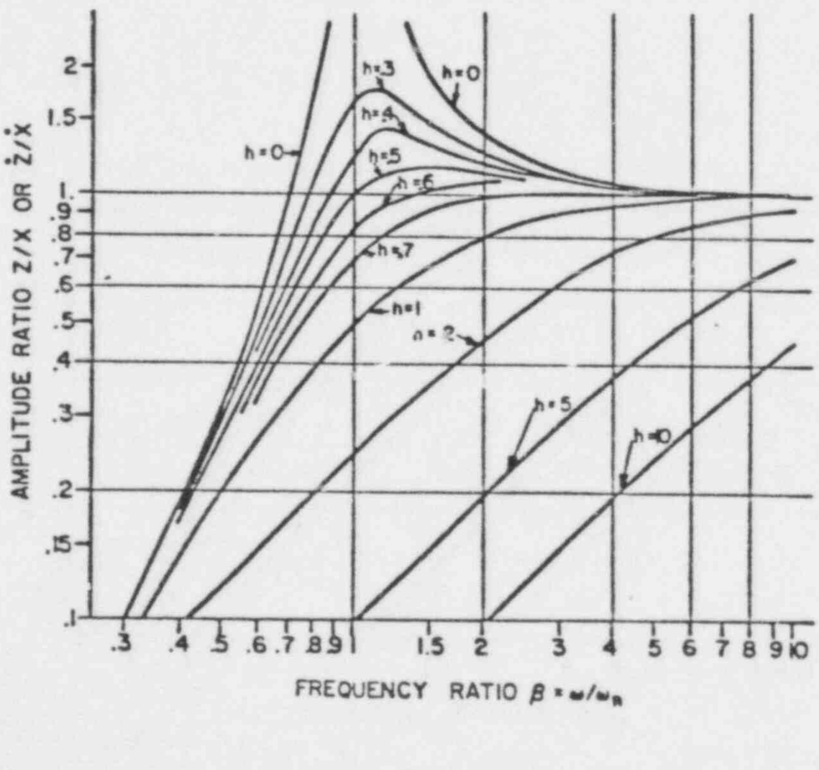

Fig. 1. Steady-state response of a seismic system to harmonic base displacement (from Reference 3).

then

$$\frac{\omega}{\omega_{n_{III}}} = 0.23.$$

From Fig. 1 (extended) $Z_I = 1.6\ X$ and $Z_{III} = 0.03\ X$. Then

$$\frac{S_{III}}{S_I} = 24 \times \frac{0.03}{1.6} \quad \text{whereupon } S_{III} = 0.45\ S_I\ .$$

Clearly the same analysis can be carried out if we work with an earthquake shaking function instead of harmonic excitation, provided we have the response curves similar to Fig. 1 in the form of a core support response spectra. In summary, if we approach the problem by assuming that the effect of the RCDs is to stiffen the fuel region, then whether pin shear forces will be reduced depends upon the natural frequency of the original system and the frequency spectra of the driving function.

ESTIMATE OF FUEL COLUMN FREQUENCIES

To apply this method to the Fort St. Vrain reactor core, we will describe the response of a core column in terms of a single degree of freedom or a single coordinate so that we can estimate the fuel column natural frequencies. Because of the relatively high friction between blocks and the relatively low known and predicted earthquake acceleration values, a fuel region can be expected to respond as seven base excited columns restrained to move together at their top (Fig. 2).

We can describe the lowest mode response for this system in terms of the tip response $Z(t)$ relative to the base excitation $v_g(t)$. Let the absolute displacement of a fuel column be $v^a(x,t)$. Let the displacement of a point on the column relative to the base be $w(x,t)$ (see Fig. 2). We will assume the predominate response to be in the first mode, and write

$$v^a(x,t) = v_g + w(x,t)$$

1836 012

and that $w(x,t) = \Psi(x)\, Z(t)$

where $\psi(x)$ is an admissible shape function. By writing the kinetic and potential energy expressions for all effects that we may wish to include, and applying Hamilton's principle to the result we can develop an equation of motion of the form

$$m_{eff}\ Z(t) + k_{eff}\ Z(t) = -\ m_g\ v_g(t) - p_{eff}(t)$$

where m_{eff} = the effective mass

k_{eff} = the effective stiffness

p_{eff} = the effective loading.

In this analysis, we will include a number of different terms in the effective stiffness so that we can assess their relative effects on the response. Thus, in the above equation

$$k_{eff} = k_b - k_g - k_a - k_p + k_{sc}$$

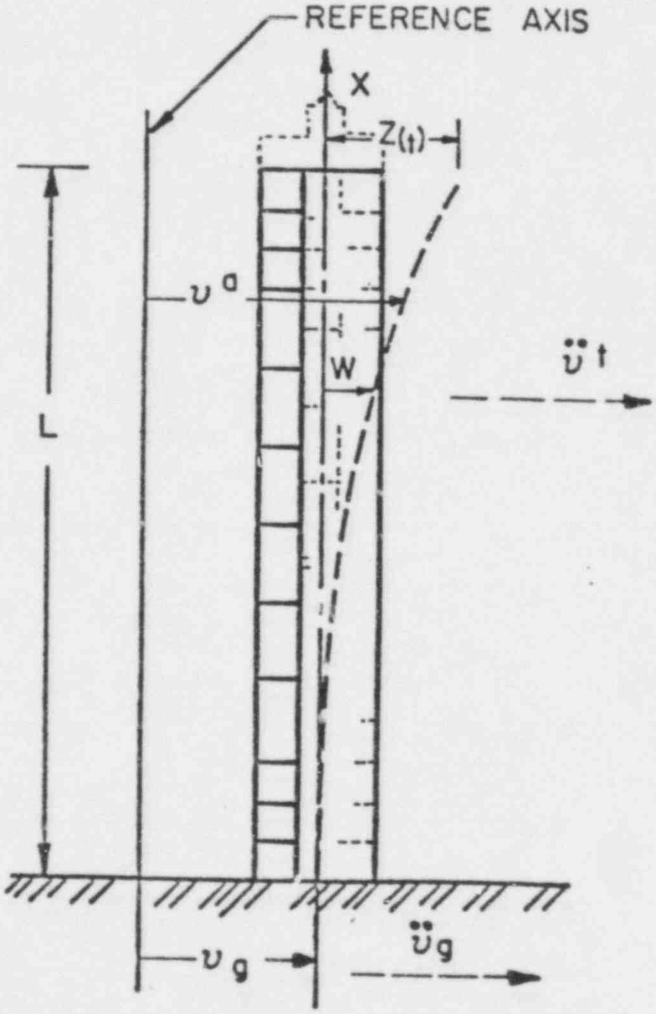

Fig. 2. Motion of a fuel region.

where

$$k_b = EI \int_0^L \left[\Psi''(x)\right]^2 dx$$

is the bending stiffness of the column, and

$$k_g = \int_0^L W(x) \left[\Psi'(x)\right]^2 dx$$

is the geometric stiffness ($W(x)$ is the axial load as a function of the length because of the weight of the column). The term

$$k_a = N \int_0^L \left[\Psi'(x)\right]^2 dx$$

is an added geometric stiffness term accounting for the constant axial load (N) that occurs because of the keyed plenum blocks, RCDs, etc. The term

$$k_p = \int_0^L q(x) \left[\Psi(x)\right]^2 dx$$

is a stiffness effect because of the lateral pressure $q(x)$ across a fuel column. The term

$$k_{sc} = \frac{\alpha^2 E^2 I^2}{A G} \int_0^L \left[\Psi'''(x)\right]^2 dx$$

is a term that represents the shear stiffness of the column. The two te ms m_{eff} and m_g given by

$$m_{eff} = \int_0^L m(x) \left[\Psi(x)\right]^2 dx$$

$$m_g = \int_0^L m(x) \left[\Psi(x)\right] dx$$

represent an effective mass for the fuel column and a mass like term to convert the base motion to an effective force, respectively. In the above

E	=	Young's modulus for graphite
I	=	the cross sectional moment of inertia
q(x)	=	the lateral pressure loading on the column
α	=	the geometric shear correction factor
A	=	the cross sectional area of a fuel column
G	=	the shear modulus of elasticity
m(x)	=	the mass per unit column length.

By including all these terms separately, we can assess their relative effects on the undamped natural frequency and bound the possible frequencies such that the method that has been described can be applied.

Table I gives the result of carrying out the details of the analysis with $\Psi(x) = 1 - \cos(\pi X/2L)$, where

$$\omega = \sqrt{\frac{k_{eff}}{m_{eff}}} \quad .$$

We have also included the irradiation effect on Young's modulus by taking the extreme values for H327 graphite as given in Ref. 4. Table III shows the other values of parameters used in carrying out the details of the analysis.

APPLICATION TO THE FSV CORE

Using the bounding values of natural frequency as 16 rad/sec and 29 rad/sec, and looking at the effects of the boundary conditions of cases II and III, we can compare the idealized ratios of maximum shearing stress in the new configuration (with RCDs) to the original configuration (without RCDs) during an earthquake just as in the harmonic excitation examples provided that we use the response curves for an earthquake exciting function.

TABLE III

PARAMETERS USED IN FSV COLUMN FREQUENCY CALCULATION

m_{eff} = 1.526 lb-s^2/in.
k_g = 3394 lb/in
k_b = 3.109 x 10^{-4} E lb/in
k_a = 0.6366 lb/in (with RCDs, 1.002 lb/in)
k_p = -46.3 lb/in
k_{sc} = 1.475 $(E)^2$

The response spectra for the FSV core support floor is not available. However, two spectra are available that should allow a satisfactory estimate of the relative effects of the installation of the RCDs.

The first response spectra that we have used is shown in Fig. 3 by the dashed lines. This response spectra was obtained in the following manner. The original (solid line) is for the bottom head of the PCRV of a larger plant as given in GASSAR-6[5]. This response spectra was shifted to the right (dotted line) so that the peak response occurs at a period of 0.5 sec to correspond to the measured natural period of the FSV PCRV as reported in Ref. 6. Note that because we are only interested in the relative effect of the RCDs, we are not concerned about the magnitudes in Fig. 3, and unless some very unusual "filtering" occurs leading to an extremely broad band peak response, the dotted spectra should be representative of the PCRV for the FSV plant. Table II, column 3 shows the results of the calculations using the dashed spectra of Fig. 3.

If the actual FSV core plane response spectra is shifted even further to the right on Fig. 3, the fuel column shear stresses will continue to be reduced by the installation of the RCDs with one exception. If the spectra is shifted so far to the right that point "A" (Fig. 3), is at a period of 0.22 sec (ω = 29 rad/s) or greater, then the maximum shear forces could increase by 28% provided that the original natural frequency of the fuel column (ω_I) is as high as 29 rad/s and also that the RCDs result in a pinned end condition. Such conditions are not deemed likely for this structure.

We also note that if the true response spectra is shifted to the left (Fig. 3) so that point "B" is at a period of 0.09 s or less, then the shear forces may also be increased by the installation of the RCDs.

Figure 4 shows the floor response spectra for the FSV reactor and turbine building floor slabs. The dotted line shows the previously discussed response spectra of Fig. 3 scaled down to 1.5 g. It is likely that much of the high frequency (low period) would be filtered out of a response spectra that applied only to the core support structure, and would appear much as the dashed line. However, we can use Fig. 4 as it is to estimate the effect of the RCDs on the maximum shear stresses. These results are also shown in Table II, column 3.

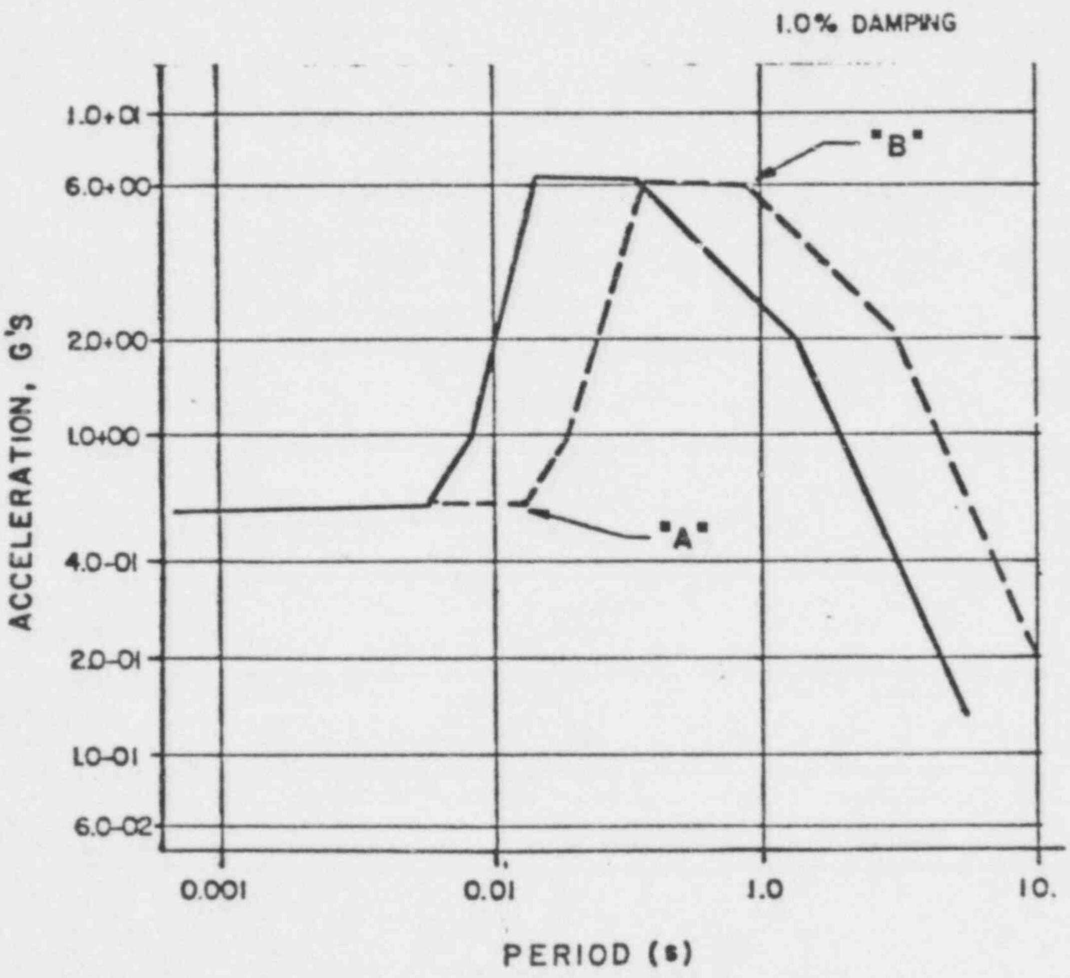

Fig. 3. Reactor bottom head horizontal response spectra for operating basis earthquake.

FUEL ELEMENT IMPACT VELOCITIES AND FORCES

Vibration studies[7,8,9] on core like structures (stacked blocks) suggest that by far the largest forces produced during a seismic event are the forces produced by impact of block against block. In the FSV reactor even though the initial response of the core may be column bending, impact between a core block column and the side wall may be expected to occur (assuming the relative displacement response is greater than the gap between a boundry column and the side wall) and once the first impact occurs it will be followed by numerous block to block impacts. The vibration studies referred to above indicate that the larger the clearance between elements the larger the impact forces.

The proposed RCDs will limit the accumulation of gaps between the fuel regions and therefore may limit the intensity of impact forces. Fig. 5 is a model of the FSV core without RCDs (case I). If we assume an impulsive ground motion to the right, the fuel region on the left (#1) will impact the permanent reflector block after undergoing a relative displacement of approximately 0.12 in. The impact sequence will then propagate from left to right. Fig. 6 is a model of the FSV core with RCDs in place (case II). If we again assume an impulsive ground motion to the right the fuel region on the right (#7) will impact on the RCD after undergoing a relative motion of approximately 0.030 in. (0.150-0.120). The impact sequence will then propagate from right to left.

The analysis which follows illustrates the difference in the magnitude of the impact forces involved in the two cases.

Assume that the relative displacement (Z) and the relative velocity ($\dot{Z}$) of the core regions are as shown in Fig. 7. These curves represent the relative response motion that would be produced by the seismic motion $x(t)$ at the core base for the case where no contact between core regions is allowed. Now assume that in Case I (Fig. 5, no RCDs) this initial (before contact) relative motion is such that contact occurs at some point to the left of line a-a in Fig. 7, say at pt. #1; then the initial impact velocity is $\dot{Z}_1$. With the RCDs present (case II) the initial contact will occur at pt. #2 with an impact velocity of $\dot{Z}_2$. Since forces are proportional to impact velocities, forces will be reduced.

1835 018

If in case I (no RCDS) the first impact is to the right of line a-a then the effect of adding RCDs (case II) may be to either increase or decrease the impact force. However, in general, for a system capable of large relative motion excursions without stops (a "soft" system), constraint involving the smallest clearance gaps will result in the lowest impact forces. The computations previously referred to in this report for the natural frequency of the FSV fuel columns show that the FSV is a "soft system" relative to the appropriate response spectra. Consequently the addition of the RCDs can be expected to decrease the impact velocities and thus the impact forces.

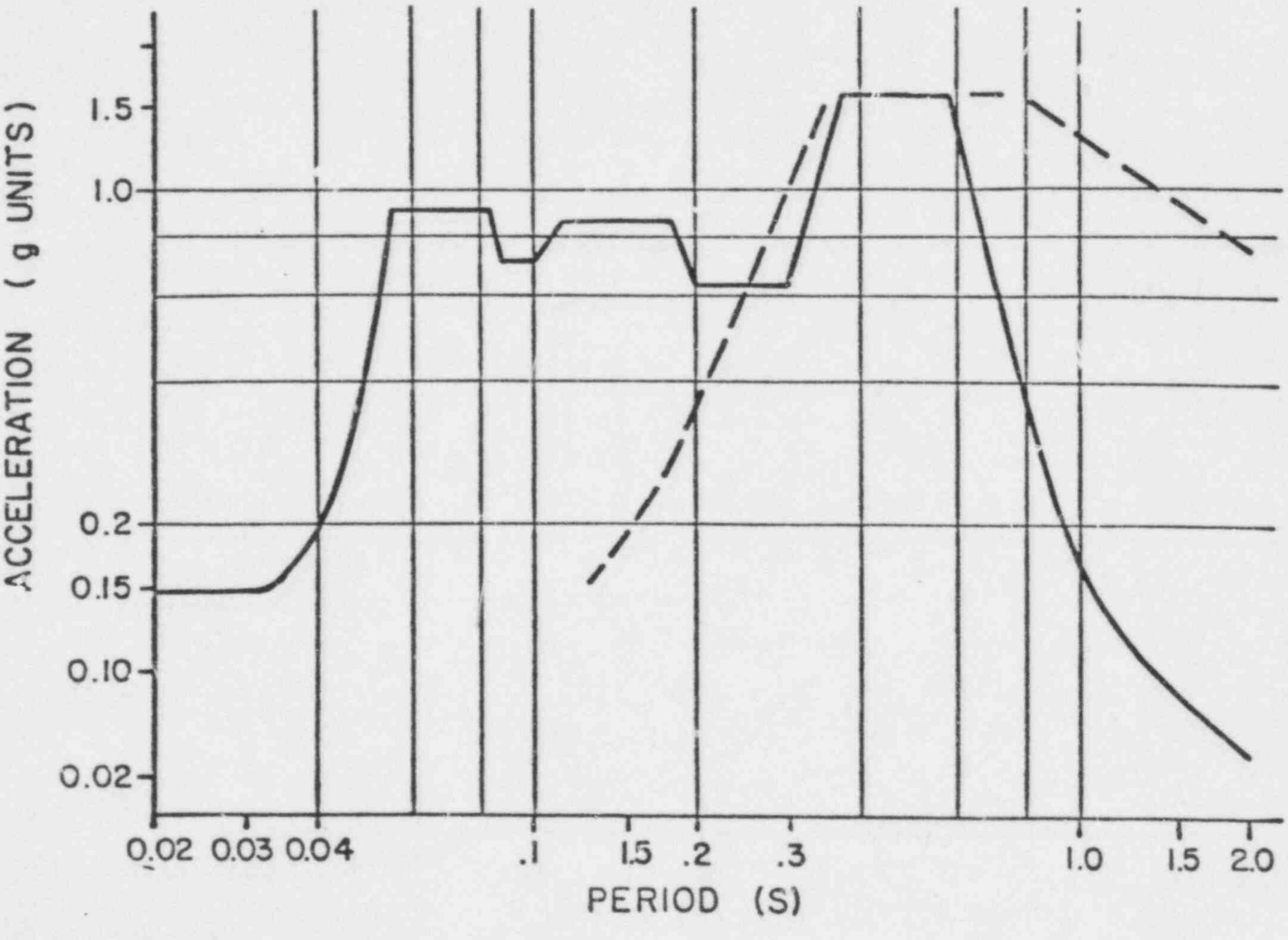

Fig. 4. Horizontal floor response spectra, safe shutdown earthquake.

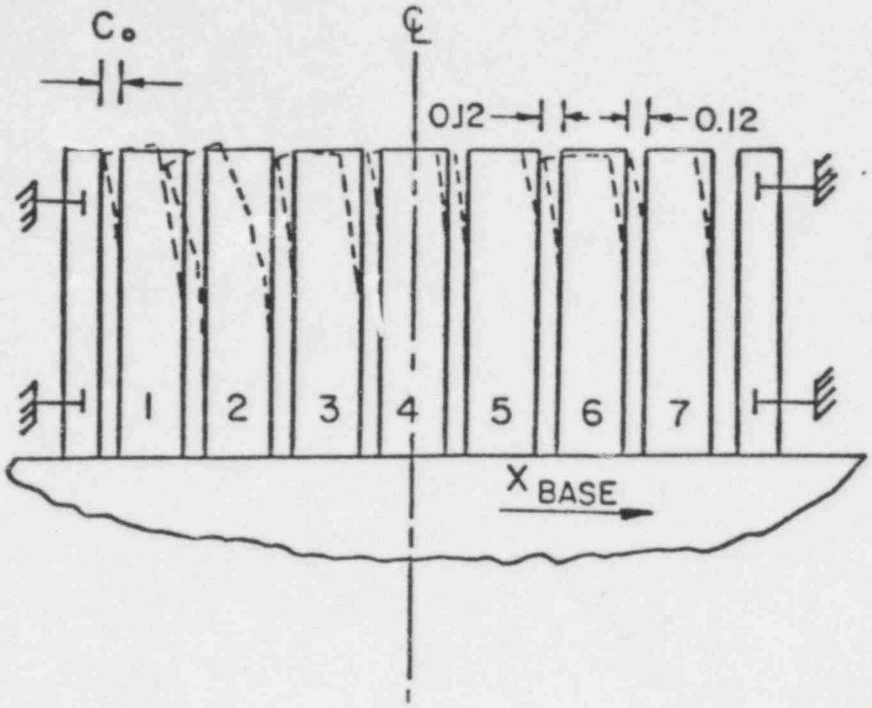

Fig. 5. Model illustrating initial impact sequence without RCDs

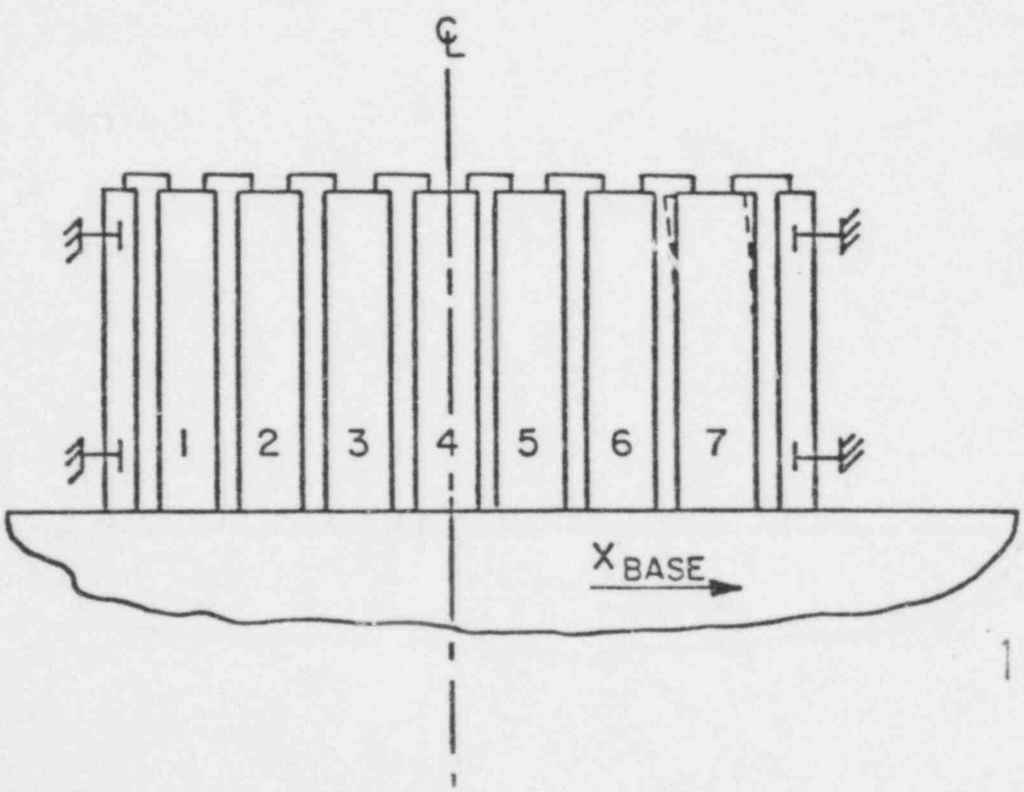

1836 020

Fig. 6. Model illustrating initial impact sequence with RCDs

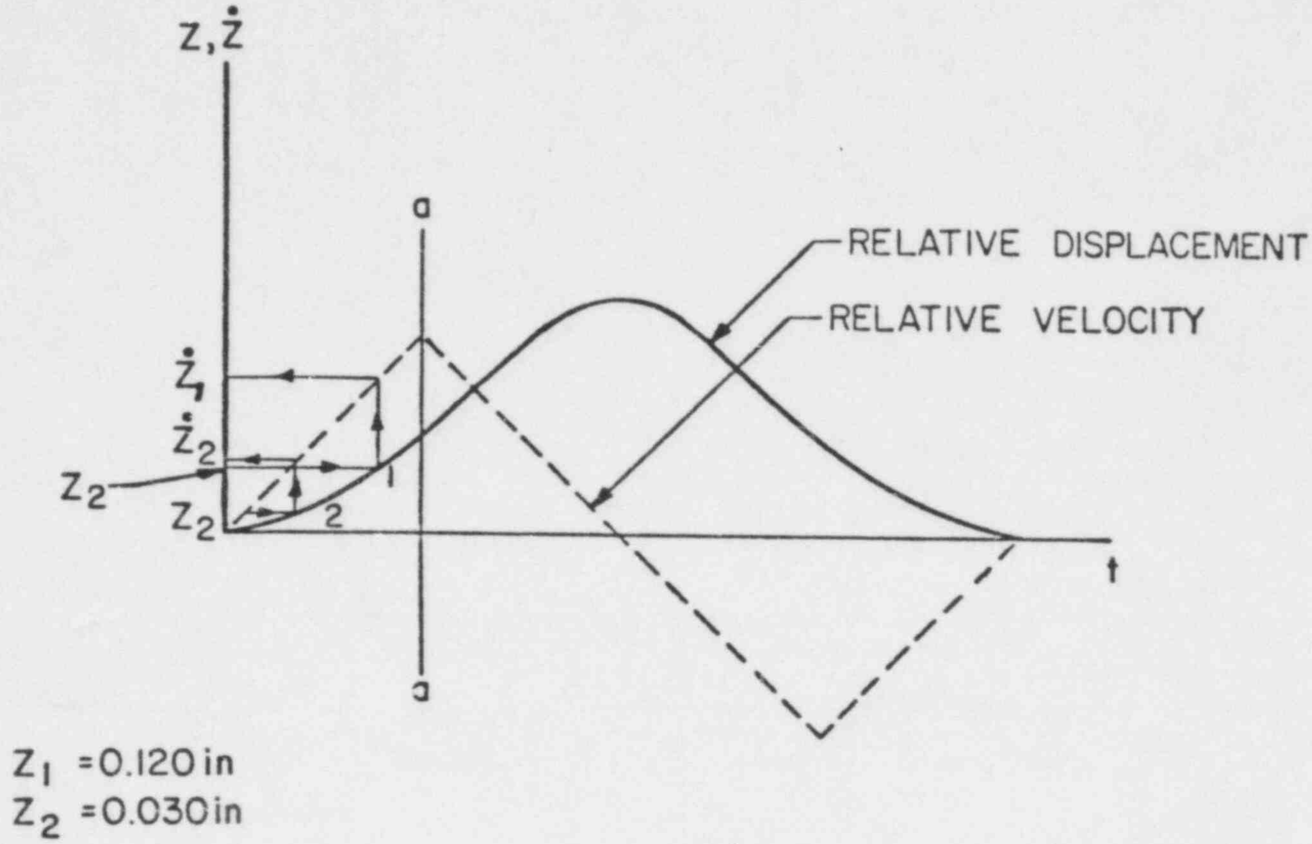

Fig. 7. Illustration for effects of increased displacement constraint on impact velocities.

REFERENCES

1. M. Stansfield, "Friction and Wear of Graphite in Dry Helium at 25, 400, and 800°C," Nuclear Applications Vol. 6, April 1969, pp. 313-320.

2. W. F. Thomson, Vibration Theory and Applications, Prentice Hall, Englewood Cliffs, NJ, 1965.

3. R. C. Dove, P. H. Adams, Experimental Stress Analysis and Motion Measurement, Charles E. Merrill Books, Inc., Columbus, Ohio, 1964.

4. R. J. Price, "Mechanical Properties of Graphite for High Temperature Gas Cooled Reactors: A Review," General Atomic Report #GA A13524 - UC77, Sept. 22, 1975.

5. GASSAR-6, General Atomic Standard Safety Analysis Report.

6. Fort St. Vrain Nuclear Generating Station - PSCo Document, "Core Fluctuation Investigation Status and Safety Evaluation Report," Aug. 1978.

7. K. D. Lathrop, Ed., "Reactor Safety and Technology Quarterly Progress Report," July 1 - Sept. 30, 1976, LA-NUREG-6579-PR, pp. 13-19.

8. J. G. Bennett, "A Physically Based Analytical Model for Predicting HTGR Core Seismic Response," Proceedings of the Japan-US Seminar on HTGR Safety Technology, BNL-NUREG-50689 - Vol. I, pp. 126-135.

9. Experimental Seismic Program for HTGR Safety as Reported in the Nuclear Reactor Safety Quarterly Progress Reports, Los Alamos Scientific Laboratory, NUREG/CR-0062 - LA-7278-PR, LA-NUREG-69-34-PR, NUREG/CR-0522 - LA-7567-PR, 1978.